THE ROYAL SOCIETY

Received 5 March 2003
Accepted 16 April 2003
Published online 8 July 2003

A feature-based model of symmetry detection

Renata Scognamillo[1,2*], Gillian Rhodes[3], Concetta Morrone[2,4] and David Burr[2,5]

[1]*Scuola Normale Superiore, Piazza dei Cavalieri, Pisa, Italy*
[2]*Istituto di Neuroscienze del CNR, Via Moruzzi 1, Pisa, Italy*
[3]*School of Psychology, University of Western Australia, Crawley, WA 6009, Australia*
[4]*Facoltà di psicologia, Università Vita-Salute San Raffaele, Via Olgettina 58, Milan, Italy*
[5]*Dipartimento di psicologia, Università di Firenze, Via S. Nicolò 89, Florence, Italy*

Symmetry detection is important for many biological visual systems, including those of mammals, insects and birds. We constructed a symmetry-detection algorithm with two stages: location of the visually salient features of the image, then evaluating the symmetry of these features over a long range, by means of a simple Gaussian filter. The algorithm detects the axis of maximum symmetry for human faces (or any arbitrary image) and calculates the magnitude of the asymmetry. We have evaluated the algorithm on the dataset of Rhodes *et al.* (1998 *Psychonom. Bull. Rev.* **5**, 659–669) and found that the algorithm is able to discriminate small variations of symmetry created by computer-manipulating the symmetry levels in individual faces, and that the values measured by the algorithm correlate well with human psycho-physical symmetry ratings.

Keywords: visual perception; symmetry; faces; local energy

1. INTRODUCTION

Human observers are very sensitive to bilateral symmetry in visual patterns (reviewed by Baylis & Driver 1995; Tyler 1996; Wagemans 1997). Rapid detection of symmetry may facilitate early visual processes, such as figure–ground segmentation (Koffka 1935; Rock 1983; Driver *et al.* 1992) and contribute to later processes, such as recognition of objects from novel viewpoints (Vetter *et al.* 1994; Kovacs *et al.* 1998). In addition to detecting perfect symmetry, we can also discriminate subtle deviations from perfect symmetry (Wagemans 1997). This ability may help direct our attention to interesting and potentially important objects in our immediate environment, such as when we follow the direction of another person's averted (asymmetric) gaze (Vecera & Johnson 1995; Driver *et al.* 1999).

The ability to detect symmetry and to discriminate subtle deviations from perfect symmetry may also play a part in biologically significant decisions, such as mate selection. Like many animals, humans find symmetry attractive in potential mates (Møller & Swaddle 1997; Thornhill & Gangestad 1999). Attractiveness and mate appeal ratings increase with facial symmetry, and these ratings are generally highest when facial asymmetries are eliminated altogether (Rhodes *et al.* 1998; Perrett *et al.* 1999). Studies that have failed to find that perfectly symmetric faces are attractive have either used flawed methods of creating symmetric faces (e.g. Kowner 1996) or have failed to control for expression (Swaddle & Cuthill (1995) and see Little *et al.* (2002) for a recent review). Nor does the appeal of symmetry appear to be due to correlations with other attractive traits, such as averageness (Rhodes *et al.* 1999) or sexual dimorphism (Penton-Voak *et al.* 2001). Finally, we note that some authors have questioned the appeal of symmetry, because attractiveness correlates with symmetry even when only hemifaces are shown (Scheib *et al.* 1999; Penton-Voak *et al.* 2001). However, this concern assumes that hemifaces do not contain cues to symmetry, which is not true. For example, the amount of nose and mouth visible in a hemiface indicates whether those features are symmetrically (centrally) located.

Individuals with symmetric bodies are also more successful in attracting mates than their asymmetric peers (see Thornhill & Gangestad 1994). The functional significance of this preference for symmetric mates is controversial. It may help identify high-quality mates, because symmetry signals developmental stability and health (Møller & Swaddle 1997), or it may be a by-product of simple information processing mechanisms, such as generalization gradients (Enquist & Johnstone 1997). Either way, our ability to make subtle discriminations between different levels of symmetry in faces can influence important life decisions.

The biological importance of symmetry, the possible contribution of symmetry detection to early visual processes like figure–ground segmentation and the fact that many biological visual systems, including those of insects and birds, are sensitive to symmetry (Lehrer *et al.* 1994; Swaddle & Cuthill 1994*a*,*b*; Moller 1995) suggest that there may be specialized symmetry-detection mechanisms in mammalian visual systems.

Given that symmetry detection is an important aspect of human and animal vision, it seems likely that visual systems have evolved to detect symmetry efficiently. Here, we propose a quantitative two-stage model of symmetry detection and test the model against human performance in symmetry rating of faces. We have adapted the 'local energy' model of feature detection (Morrone & Burr 1988) to localize the vertical symmetry axis of a human face (or any other object) and estimate the amount of

*Author for correspondence (r.scognamillo@sns.it).

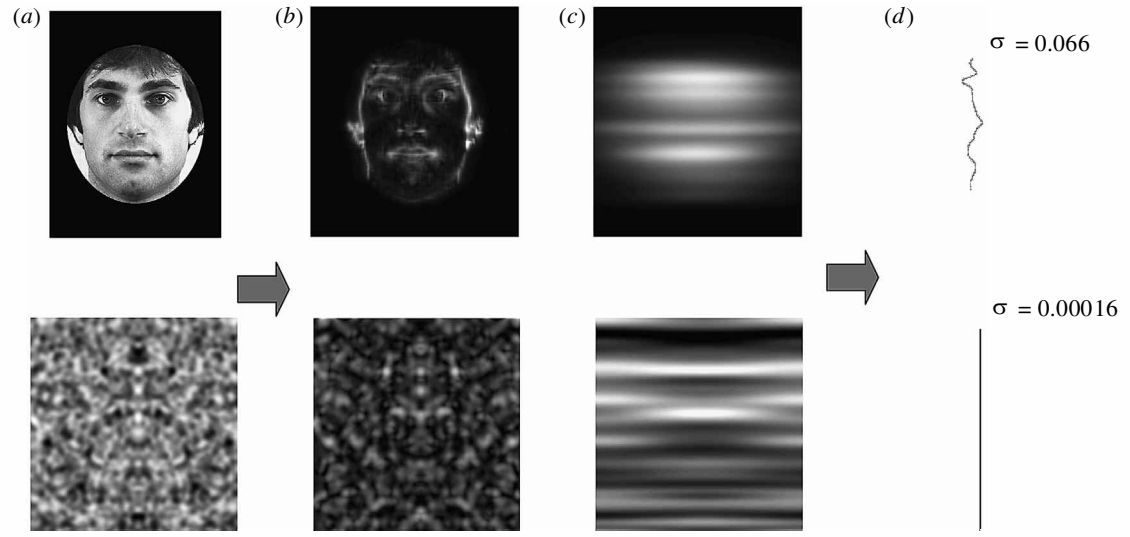

Figure 1. Illustration of the algorithm for detecting symmetry in a human face (upper figures) and an artificial pattern produced by symmetrically reflecting a random noise pattern about the vertical axis. (*a*) This shows the original stimuli. The local energy profile (*b*) is extracted, following the details given in § 2 (equations (2.1)–(2.5)). This energy profile is then convolved with a Gaussian filter (equation (2.6)) to produce (*c*), from which the positions of local maxima are determined row by row to locate the symmetry axis (*d*). The asymmetry value assigned to the image is given by the weighted standard deviation of the maxima position divided by the normalization factor ρ.

deviation from perfect symmetry. The model was originally introduced to detect salient features in an image, such as edges, lines or combinations of the two (Morrone & Burr 1988; Burr & Morrone 1990). These features are revealed as local maxima of the 'energy function' of the two-dimensional (2D) image. In this application the model is used to highlight features for subsequent evaluation of symmetry by a second-stage filter.

2. METHODS: ALGORITHM

The algorithm operates in two stages. The first stage calculates a 2D local energy function that defines a sketch of the image, where visual features assume a positive value proportional to their salience. The second stage evaluates the symmetry of this energy sketch by convolving it with a broad Gaussian filter, and then localizing the local maxima. The process is illustrated in figure 1, both for a human face and an artificial image made up from random noise.

The local energy of an image $E(x)$ is obtained by first convolving the image with operators of even symmetry and odd symmetry, then combining these two outputs (O_e and O_o) by Pythagorean sum to produce an all-positive image with maxima at salient features:

$$E(x) = \sqrt{O_e(x)^2 + O_o(x)^2}, \tag{2.1}$$

where O_e and O_o are obtained by convolving the original image with even- and odd-symmetric filters G_e and G_o:

$$O_e(x) = \int G_e(x - \xi) I(\xi) \mathrm{d}\xi, \tag{2.2}$$

$$O_o(x) = \int G_o(x - \xi) I(\xi) \mathrm{d}\xi.$$

The two filters G_e and G_o have the same amplitude spectrum but are in quadrature phase (so that they are orthogonal in L^2 space). The phase is chosen so they have an even and odd symmetry about a given preferred orientation u. Their amplitude spectrum follows a Gaussian function of log spatial frequency, approximating the spatial frequency tuning functions of human vision:

$$a(u,w) = \exp(-\ln^2(|u|/p)/2s_u^2)\exp(-w^2/2s_w^2), \tag{2.3}$$

where w is the direction orthogonal to u, and p, s_u and s_w are suitably defined constants. The function is a parabola along u on a log–log plot with a peak corresponding to p and a half bandwidth corresponding to s_u log units at half-height.

As a consequence of the orthogonality of O_e and O_o, salient features in the image are identified with the 'local maxima' of the energy function $E(x)$ associated with various pairs of filters having different symmetry orientations and spatial scales. The local maxima may be detected along the direction of steepest gradient of the energy function. The nature of the feature (edge, line or a combination of both) is given by the argument $A(x)$:

$$A(x) = \arctan(O_e(x)/O_o(x)). \tag{2.4}$$

For lines the argument is near 0, for edges $\pi/2$.

The first stage of the symmetry algorithm is to calculate the local energy profiles $E_v(x)$, $E_h(x)$ of the image with respect to two orientations (vertical and horizontal) and one spatial scale, defined by $p = 32$ cycles per picture, $s_u = 1$ log unit, $s_w = 16$ cycles per picture (see equation (2.3) above). This scale may be considered to be the most relevant for face discrimination as p corresponds to a peak frequency of 10.3 cycles per face unit, near the most efficient range (Fiorentini *et al.* 1983; Hayes *et al.* 1986). s_u is the full-bandwidth at half height of 3.4 octaves and s_w the orientation full-bandwidth at half height of 98°. In previous implementations of the model we have used four different spatial scales and four different orientations (Burr & Morrone 1990). However, as it has been shown that the energy model works acceptably well with a single broad spatial scale and two broad orthogonal orientations (Morrone & Owens 1987), we use this implementation here to limit the complexity of the algorithm. A single representation of the image features is obtained by simply summing the two orthogonal energy functions:

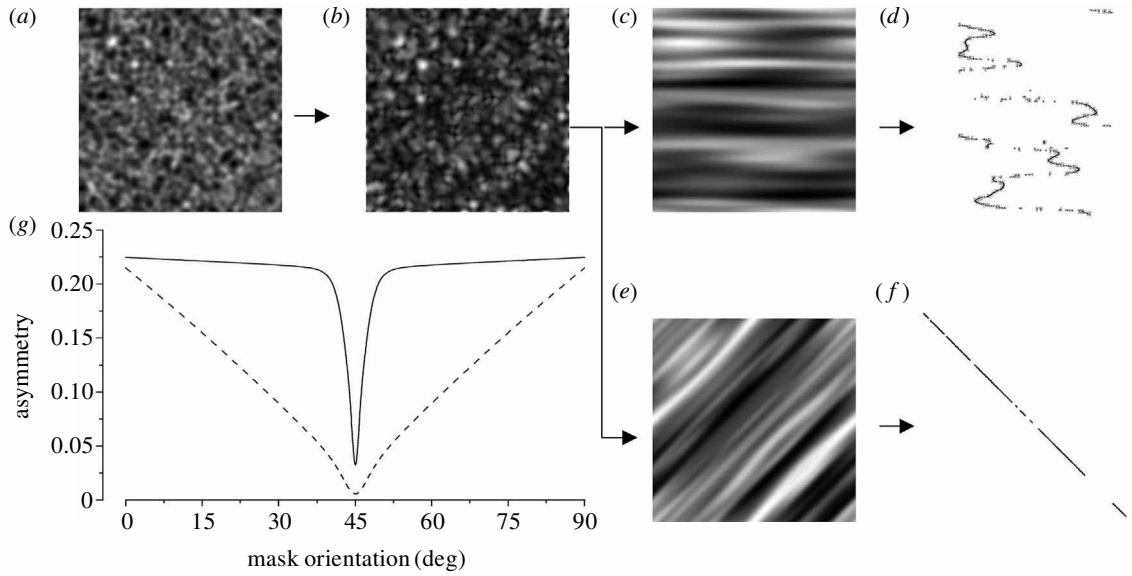

Figure 2. Detection of non-vertical symmetry. (*a*) A random-dot pattern reflected about the 45° diagonal. (*b*) The energy map of (*a*). (*c*) This shows the convolution with a vertical second-stage filter like that used in figure 1. (*d*) This shows the line-by-line maxima of this output, clearly highly asymmetrical. (*e*) This shows the output of a second-stage filter applied to (*b*) of appropriate orientation (45°), together with the maxima (*f*), forming a single line along the axis of symmetry. (*g*) This shows the asymmetry measures as a function of mask orientation, for the narrow filters illustrated here and in figure 1 ($s_x/s_y = 16$, continuous line) and for a broader filter ($s_x/s_y = 1.6$, dashed line). Both filter types show a clear minimum at the axis of symmetry, easy for any algorithm to detect.

$$E = E_h(x) + E_v(x). \tag{2.5}$$

This is illustrated in figure 1*b* for a human face (upper) and random-dot symmetry (lower). To evaluate the symmetry of the feature map the summed energy E is convolved with a vertically oriented Gaussian filter spatially defined by

$$F = 1/4[\exp(-x^2/2s_x^2)\exp(-y^2/2s_y^2)], \tag{2.6}$$

where $s_x = 120$ pixels (or 0.73 face units) and $s_y = 7.5$ pixels (or 0.046 face units). The output of this convolution for the two images is shown in figure 1*c*.

Position and values of local maxima are next determined row by row. Note that usually a row in $E \otimes F$ has only one maximum, but in cases where there are more the average position and value is taken. This very rarely occurs for faces, but could occur for random images (like those of figures 1 and 2) where the point of symmetry could correspond to a local minimum rather than maximum.

The maxima of the convolution determine the symmetry axis of the original image (figure 1*d*). The asymmetry value of the image is defined as the ratio σ/ρ, where σ is the weighted standard deviation (s.d.) of the maxima positions (expressed in pixels) and ρ is a normalization factor defined by $\rho^2 = \alpha\beta$, α being the distance between the pupils and β the vertical distance from a horizontal line joining the pupils to the bottom tip of the chin for faces and to the square root of the whole area for other images. An efficient strategy to search for the optimal orientation could be to use a few broad second-stage filters and then refine the search with the narrowband filters.

The above algorithm does not assume the position of symmetry, but finds it by searching for maxima in the filtered output. The only assumption is that the axis of symmetry is vertical. However, this assumption is not an essential feature of the model. If the axis of symmetry is not known, it is sufficient to use several second-stage filters with different orientation tuning, as illustrated in figure 2. Figure 2*a* is a random-dot pattern symmetric about the 45° diagonal, and figure 2*b* the associated energy map. Figure 2*c* shows the result of convolution with a vertical second-stage filter, yielding the maxima of figure 2*d*, clearly yielding a high asymmetry estimate. However, convolution with a second-stage filter of appropriate orientation leads to very low asymmetry (figure 2*e*,*f*). Figure 2*g* shows the estimate of asymmetry as a function of the orientation of the second-stage filter. For the filters used in this study ($s_x/s_y = 16$), the function peaks sharply at 45° (solid curve). For broader filters the peak is more gradual (dashed lines illustrate a filter of $s_x/s_y = 1.6$).

In this study, we will continue to make the simplifying assumption that symmetry is around the vertical axis. However, figure 2 shows that this is not an essential limitation of the model, which could be readily extended to situations where the symmetry axis was completely unknown.

3. RESULTS: EVALUATION OF ALGORITHM

We tested the algorithm on a set of the images randomly selected from those used by Rhodes *et al.* (1998): 68 images comprising 17 faces with four different levels of symmetry produced by a morphing technique. The original digitized black-and-white photograph of a face is referred to as the 'normal' version. A perfectly symmetrical picture ('perfect' version) was created by averaging the normal version with its vertical mirror reflection. A 'high' symmetry version was created by warping the original face half way towards the 'perfect' symmetry face and a 'low' symmetry version was created by warping the original face the same distance D in the other direction (see figure 3 and Rhodes *et al.* (1998) for more details).

The asymmetry values assigned by the algorithm for the four symmetry versions of each face are shown in figure 4*a*. When the faces were perfectly symmetrical, the

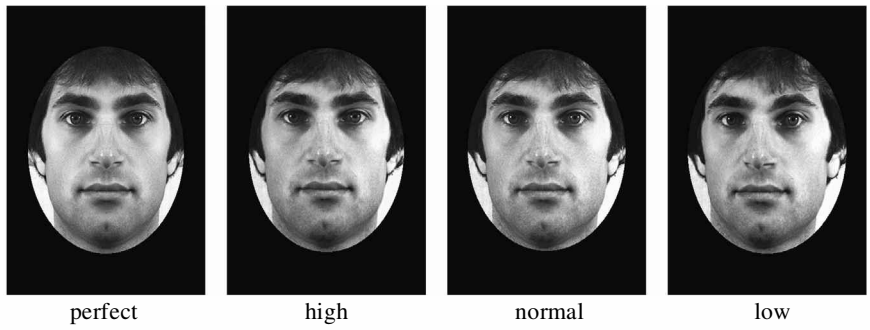

Figure 3. The four symmetry versions of a face as produced by suitable morphing techniques in Rhodes *et al.* (1998). The first on the left ('perfect version') is perfectly symmetrical. From left to right, the amount of vertical symmetry decreases each time by a fixed quantity *D*. The 'low' symmetry version is the most asymmetrical.

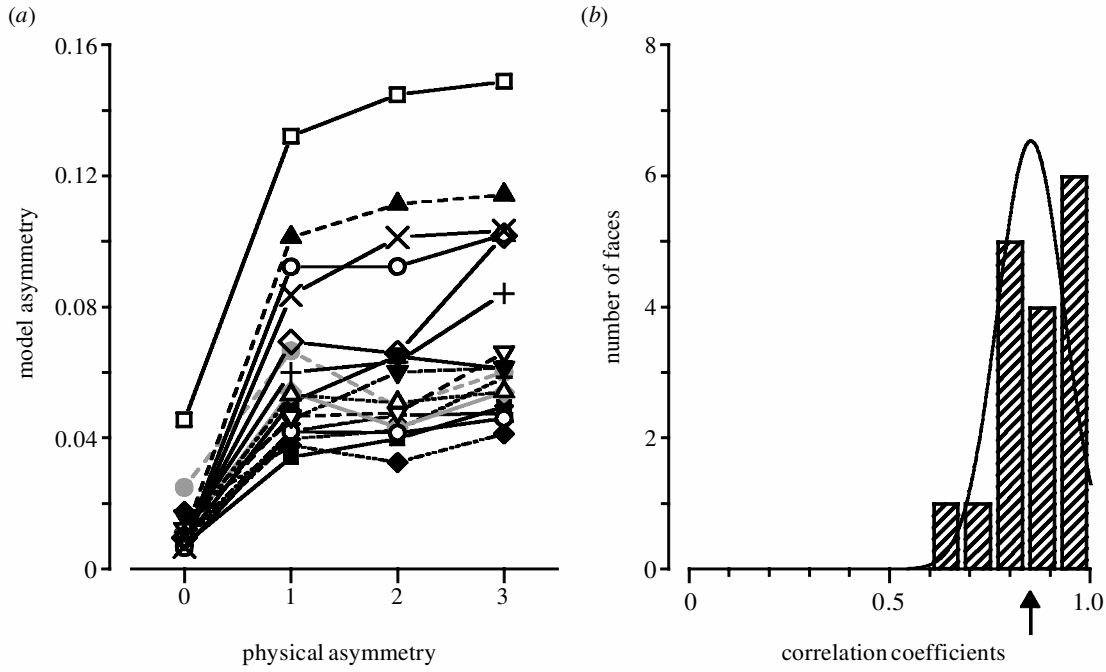

Figure 4. (*a*) Model asymmetry values for the four symmetry versions of each of the 17 faces considered (each face is represented by a different symbol). (*b*) Histogram of the correlation coefficients relating the model estimates to the physical asymmetry of the four versions of each face. The Gaussian fit has a mean of 0.85 and s.d. $\sigma = 0.1$.

algorithm gives very low asymmetry estimates, nearly 1% of the overall face. The model estimate generally increases monotonically with the physical asymmetry. Because each symmetry version varies in symmetry space by a fixed physical distance *D* from the next, it forms a metric scale, and can therefore be correlated with the model estimates. The correlation coefficients of model estimate against symmetry level for each face are summarized in the histogram of figure 4*b*. The correlations are generally good (average $r = 0.85$), attesting to the validity of the algorithm. Some violations of monotonicity can be seen between levels one and two for the model estimates. Interestingly, human observers also had difficulty discriminating these asymmetry levels (see Rhodes *et al.* 1998).

We next compared the estimates of symmetry from our model with those of human raters (Rhodes *et al.* 1998), where 64 individuals rated all faces and symmetry versions both for symmetry and for attractiveness, within the range 1–10, where 10 corresponded respectively to perfect symmetry and best attractiveness. We transformed the symmetry and attractiveness ratings to mean 'asymmetry' and 'unattractiveness' ratings by subtracting each value from 11. Figure 5*a* plots the mean asymmetry ratings against model estimates for each face. Figure 5*b* plots the histogram of all the correlation coefficients found for all faces. As is evident from both graphs, the model correlates well with the ratings (average $r = 0.91$) demonstrating a linear relation between the model and human performance.

Finally, we plotted the ratings of unattractiveness against the asymmetry estimates of the model (figure 6*a*), together with the histograms of the correlations (figure 6*b*). Here the dependency was less strong, but the average correlation was positive, $r = 0.56$.

4. DISCUSSION

We have presented a biologically plausible model of symmetry detection that performs well on both artificial and natural images and parallels human performance. The model's performance correlated well with physical manipulations of the symmetry of a set of images of faces. It also correlated well with human rating estimates of the

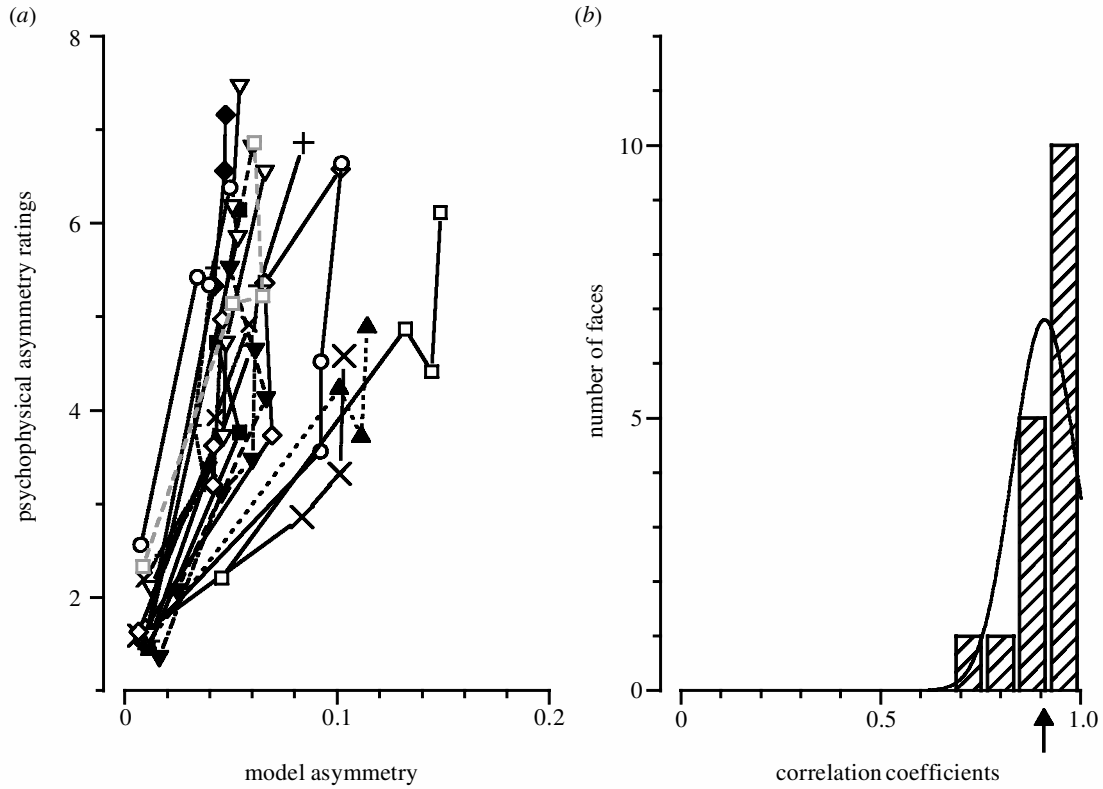

Figure 5. (*a*) Psychophysical mean asymmetry ratings of the four symmetry versions of each face (data from Rhodes *et al.* 1998) versus the corresponding model asymmetry estimates (as in figure 4*a*). Each face is represented by a different symbol. (*b*) Histogram of the correlation coefficients relating the model estimates of the four symmetry versions of each face versus the corresponding psychophysical mean asymmetry ratings. The Gaussian fit has a mean of 0.91 and s.d. $\sigma = 0.08$.

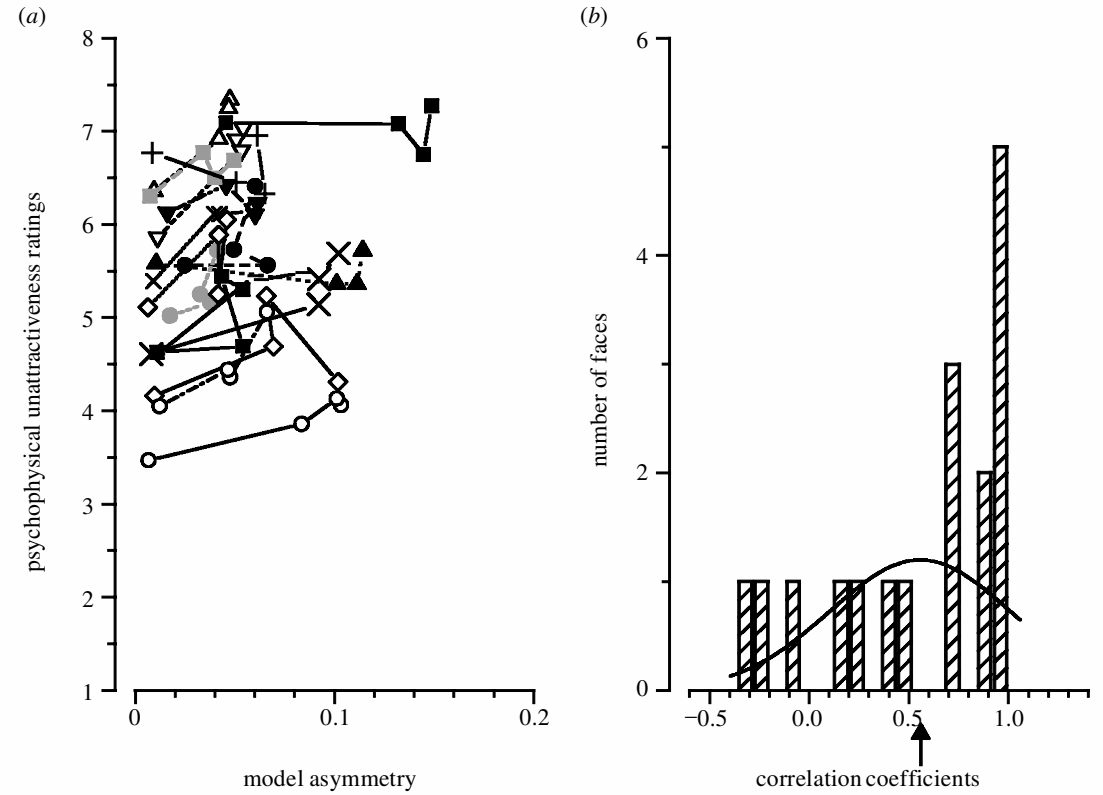

Figure 6. (*a*) Psychophysical mean unattractiveness ratings of the four symmetry versions of each face (data from Rhodes *et al.* 1998) versus the corresponding model asymmetry estimates. Each face is represented by a different symbol. (*b*) Histogram of the correlation coefficients relating the model estimates of the four symmetry versions of each face versus the corresponding psychophysical mean unattractiveness ratings. The Gaussian fit has a mean of 0.56 and s.d. $\sigma = 0.45$.

symmetry of the same images, showing it can emulate human performance with reasonable accuracy. The model requires no complicated or unrealistic biological machinery. The first stage of local energy calculation, discussed in detail elsewhere (Morrone & Burr 1988), is achieved by mechanisms resembling complex cortical cells. The additional Gaussian smoothing and the peak detection operation are both operations easily achieved by visual neural populations, particularly those of higher stages with large receptive fields.

The algorithm was designed for use with human faces, but it generalizes well to other images, such as random-dot images. We chose the random-dot patterns of figures 1 and 2 because they are a severe test of the model, being the most 'artificial' stimulus we could devise. The noise was completely uncorrelated (apart from the mirror reflection), producing no clear features in the energy map of figure 1*b*. But, the model predicted perfect symmetry for this perfectly symmetrical artificial stimulus.

In the current implementation of the model, we use only one (vertical) orientation for the second-stage filter, both to simplify the algorithm and to simulate the human observers, who were asked to evaluate vertical symmetry. However, we also illustrate a simple extension of the model, by using a series of second-stage Gaussian filters of various orientations. The orientation corresponding to the axis of symmetry shows a clear minimum, easy to identify. With this simple extension the model could both identify and evaluate symmetry along any orientation.

Dakin & Watt (1994) showed that spatially unweighted correlation models cannot explain human symmetry perception. Symmetry detection necessarily involves comparison of detailed (high-frequency) features over relatively large distances. A single linear filter large enough to straddle the distance between the features will necessarily blur out the image detail essential for symmetry (see also Tyler *et al.* 1995). Dakin & Watt (1994) concluded that filtering in combination with a feature alignment measure is useful both as a way of extracting symmetry from natural images and as an explanation for psychophysical detection of bilateral symmetry.

In our model, the nonlinearity of the local energy process serves this purpose by first transforming the image into a positive function corresponding to visually salient features. The second stage large-scale filter operates on the feature map, rather than the high-frequency details themselves, so low-pass filtering does not obliterate these marked features.

In previous studies, it has been demonstrated that our local energy model is reasonably robust in conditions of unequal lighting and shading, in that it does not respond to gradual changes in luminance, but only to features such as lines and edges. This is a useful property for a model of symmetry detection, as a gradient could distort symmetry estimates. Oblique lighting can cast harsh shadows, and these would certainly be a problem for our model, although light shadows generating widely spaced Mach bands should not be a problem for the present model given that they are detected by the energy model only by filters of very high spatial frequency preference (Ross *et al.* 1989). However, as the psychophysical measures of symmetry and attractiveness were made in conditions of fairly uniform lighting, we restricted our study to these images. It may be an interesting extension to study what types of shading affect the symmetry output of the model, and whether this follows human performance, both of symmetry estimation and of beauty.

The idea of applying the local energy model to symmetry detection so that symmetry should be determined by visual salient features rather than local variation of luminance was first proposed by Osorio (1996). Osorio also calculates the squared output of even and odd-symmetric operators, but rather than evaluating local maxima, he ranks the symmetry of each point at the local maxima of the even output. Although this has the advantage of ensuring that symmetry estimation is based on feature matching rather than local luminance calculation, there are two major drawbacks: the algorithm leads to many false positives, arising mainly from local symmetry of isolated features; and odd-symmetric features, such as face edges, or features of mixed symmetry (often resulting from oblique illumination) do not contribute to the evaluation of symmetry.

Symmetry detection has been studied psychophysically for many years (e.g. Julesz 1966), but little is known about its neural basis. Tyler & Baseler (1998) have used functional magnetic resonance imaging to identify areas in the human brain sensitive to symmetry, contrasting blood oxygenated level-dependent (BOLD) signals generated by symmetric and random patterns. In their study, early retinotopic visual areas (V1, V2, V3, V3a V4v, V5) showed very little differential response to symmetric versus random patterns. Pronounced BOLD signals were, however, found in the middle occipital gyrus. Activation was not observed in the fusiform and lingual gyri, which are known to respond to faces and objects rather than to non-object textures (Kanwisher 2000). Norcia *et al.* (2002) have recently shown that the visual evoked potential response to symmetric/random sequences was indistinguishable from that for random/random sequences up to *ca.* 220 ms, after which the response to symmetric patterns became relatively more negative. Symmetry in random-dot patterns thus appears to be extracted after an initial response phase that is indifferent to configuration.

Both these physiological results are consistent with the hypothesis that the symmetry property is extracted by processing in extrastriate cortex (Lee *et al.* 1998; Tyler & Baseler 1998). Our second-stage Gaussian filter may be modelling this higher neural process.

Interestingly, the model estimates of symmetry also correlated with estimates of attractiveness. This correlation was not strong, and the variance accounted for was clearly a small proportion of the total variance, but the same is true for correlations between human judgements of symmetry and attractiveness. The present result is, therefore, in keeping with evidence that although symmetry may contribute towards attractiveness, it is not the only determining factor (for a recent review see Rhodes & Zebrowitz (2002)).

We have shown that a simple, biologically plausible model of asymmetry estimation generates estimates that closely match those of human observers. This model may account for the widespread sensitivity to symmetry in a wide range of mammalian visual systems.

This work was supported by grants from the Italian Ministry of Education and Research (MUIR coffin2000 and coffin2001), and from the Australian Research Council to G.R.

REFERENCES

Baylis, G. C. & Driver, J. 1995 Obligatory edge assignment in vision: the role of figure and part segmentation in symmetry detection. *J. Exp. Psychol. Hum. Percept. Perform.* **21**, 1323–1342.

Burr, D. C. & Morrone, M. C. 1990 Edge detection in biological and artificial visual systems. In *Vision: coding and efficiency* (ed. C. Blakemore), pp. 185–194. Cambridge University Press.

Dakin, S. C. & Watt, R. J. 1994 Detection of bilateral symmetry using spatial filters. *Spatial Vision* **8**, 393–413.

Driver, J., Baylis, G. C. & Rafal, R. D. 1992 Preserved figure-ground segregation and symmetry perception in visual neglect. *Nature* **360**, 73–75.

Driver, J., Davis, G., Ricciardelli, P., Kidd, P., Maxwell, E. & Baron-Cohen, S. 1999 Gaze perception triggers reflexive spatio-temporal orienting. *Visual Cogn* **5**, 509–540.

Enquist, M. & Johnstone, R. A. 1997 Generalization and the evolution of symmetry preferences. *Proc. R. Soc. Lond.* B **264**, 1345–1348. (DOI 10.1098/rspb.1997.0186.)

Fiorentini, A., Maffei, L. & Sandini, G. 1983 The role of high spatial frequencies in face perception. *Perception* **12**, 195–201.

Hayes, A., Morrone, M. C., Burr, D. C. & Ross, J. 1986 Recognition of positive and engative bandpass-filtered images. *Perception* **15**, 595–602.

Julesz, B. 1966 Binocular disappearance of monocular symmetry. *Science* **153**, 657–658.

Kanwisher, N. 2000 Domain specificity in face perception. *Nature Neurosci.* **3**, 759–763.

Koffka, K. 1935 *Principles of Gestalt psychology*. New York: Harcourt Brace.

Kovacs, I., Feher, A. & Julesz, B. 1998 Medial-point description of shape: a representation for action coding and its psychophysical correlates. *Vision Res.* **38**, 2323–2333.

Kowner, R. 1996 Facial asymmetry and attractiveness judgment in developmental perspective. *J. Exp. Psychol. Hum. Percept. Perform.* **22**, 662–675.

Lee, T. S., Mumford, D., Romero, R. & Lamme, V. A. 1998 The role of the primary visual cortex in higher level vision. *Vision Res.* **38**, 2429–2454.

Lehrer, M., Horridge, G. A., Zhang, S. W. & Gadgagkar, R. 1994 Shape vision in bees: innate preference for flower-like patterns. *Phil. Trans. R. Soc. Lond.* B **347**, 123–137.

Little, A. C., Penton-Voak, I. S., Burt, M. & Perrett, D. I. 2002 Evolution and individual differences in the perception of attractiveness: how cyclic hormonal changes and self-perceived attractiveness influence female preferences for male faces. In *Facial attractiveness: evolutionary, cognitive and social perspectives* (ed. G. Rhodes & L. A. Zebrowitz), pp. 59–90. Westport, CT: Ablex.

Moller, A. P. 1995 Bumble-bee preference for symmetrical flowers. *Proc. Natl Acad. Sci. USA* **92**, 2288–2292.

Møller, A. P. & Swaddle, J. P. 1997 *Asymmetry, developmental stability and evolution*. Oxford University Press.

Morrone, M. C. & Burr, D. C. 1988 Feature detection in human vision: a phase-dependent energy model. *Proc. R. Soc. Lond.* B **235**, 221–245.

Morrone, M. C. & Owens, R. 1987 Feature detection from local energy. *Pattern Rec. Lett.* **1**, 103–113.

Norcia, A. M., Candy, T. R., Pettet, M. W., Vildavski, V. Y. & Tyler, C. W. 2002 Temporal dynamics of the human response to symmetry. *J. Vision* **2**, 132–139.

Osorio, D. 1996 Symmetry detection by categorization of spatial phase, a model. *Proc. R. Soc. Lond.* B **263**, 105–110.

Penton-Voak, I. S., Jones, B. C., Little, A. C., Baker, S., Tiddeman, B., Burt, D. M. & Perrett, D. I. 2001 Symmetry, sexual dimorphism in facial proportions and male facial attractiveness. *Proc. R. Soc. Lond.* B **268**, 1617–1623. (DOI 10.1098/rspb.2001.1703.)

Perrett, D. I., Burt, D. M., Penton-Voak, I. S., Lee, K. J., Rowland, D. A. & Edwards, R. 1999 Symmetry and human facial attractiveness. *Evol. Hum. Behav.* **20**, 295–307.

Rhodes, G. & Zebrowitz, L. A. (eds) 2002 *Facial attractiveness: evolutionary, cognitive and social perspectives*. Westport, CT: Ablex.

Rhodes, G., Proffitt, F., Grady, J. M. & Sumich, A. 1998 Facial symmetry and the perception of beauty. *Psychonom. Bull. Rev.* **5**, 659–669.

Rhodes, G., Sumich, A. & Byatt, G. 1999 Are average facial configurations only attractive because of their symmetry? *Psychol. Sci.* **10**, 52–58.

Rock, I. 1983 *The logic of perception*. Cambridge, MA: MIT Press.

Ross, J., Morrone, M. C. & Burr, D. C. 1989 The conditions for the appearance of Mach bands. *Vision Res.* **29**, 699–715.

Scheib, J. E., Gangestad, S. W. & Thornhill, R. 1999 Facial attractiveness, symmetry and cues of good genes. *Proc. R. Soc. Lond.* B **266**, 1913–1917. (DOI 10.1098/rspb.1999.0866.)

Swaddle, J. P. & Cuthill, I. C. 1994*a* Female zebra finches prefer males with symmetrical chest plumage. *Proc. R. Soc. Lond.* B **258**, 267–271.

Swaddle, J. P. & Cuthill, I. C. 1994*b* Preference for symmetric males by female zebra finches. *Nature* **367**, 165–166.

Swaddle, J. P. & Cuthill, I. C. 1995 Asymmetry and human facial attractiveness: symmetry may not always be beautiful. *Proc. R. Soc. Lond.* B **261**, 111–116.

Thornhill, R. & Gangestad, S. W. 1994 Human fluctuating asymmetry and sexual behavior. *Psychol. Sci.* **5**, 297–302.

Thornhill, R. & Gangestad, S. W. 1999 Facial attractiveness. *Trends Cogn. Sci.* **3**, 452–460.

Tyler, C. W. 1996 *Human symmetry perception and its computational analysis*. Utrecht, The Netherlands: VSP BV.

Tyler, C. W. & Baseler, H. 1998 A. 1998 Properties of the middle occipital gyrus: an fMRI study. *Soc. Neurosci. Abstr.* **24**, 1507.

Tyler, C. W., Hardage, L. & Miller, R. T. 1995 Multiple mechanisms for the detection of mirror symmetry. *Spatial Vision* **9**, 79–100.

Vecera, S. P. & Johnson, M. H. 1995 Gaze detection and the cortical processing of faces: evidence from infants and adults. *Visual Cogn.* **2**, 59–87.

Vetter, T., Poggio, T. & Bulthoff, H. H. 1994 The importance of symmetry and virtual views in three-dimensional object recognition. *Curr. Biol.* **4**, 18–23.

Wagemans, J. 1997 Characteristics and models of human symmetry detection. *Trends Cogn. Sci.* **1**, 346–352.

As this paper exceeds the maximum length normally permitted, the authors have agreed to contribute to production costs.